Angular analysis of the decay $B^0 \rightarrow K^{*0}\mu^+\mu^-$ with CMS

Mauro Dinardo*†

INFN and Unversity of Milano Bicocca

E-mail: mauro.dinardo@cern.ch

The angular distributions and the differential branching fraction of the decay $B^0 \rightarrow K^*(892)^0\mu^+\mu^-$ are studied using data corresponding to an integrated luminosity of 20.5 fb$^-$1 collected with the CMS detector at the LHC in pp collisions at $\sqrt{s} = 8$ TeV. From 1430 signal decays, the forward-backward asymmetry of the muons, the $K^*(892)^0$ longitudinal polarization fraction, and the differential branching fraction are determined as a function of the dimuon invariant mass squared. The measurements are among the most precise to date and are in good agreement with standard model predictions.

---

*Speaker.

†A footnote may follow.

Phenomena beyond the standard model (SM) of particle physics can manifest themselves directly, via the production of new particles, or indirectly, by affecting the production and decay of SM particles. Analyses of flavor-changing neutral current (FCNC) decays are particularly sensitive to the effect of new physics, since such decays are highly suppressed in the SM. The FCNC decay, $B^0 \rightarrow K^{*0}\mu^+\mu^-$ (K^{*0} indicates the $K^*(892)^0$, and charge conjugate states are implied for all particles unless stated otherwise), provides many opportunities to search for new phenomena. In addition to the branching fraction, other properties of the decay can be measured, including the forward-backward asymmetry of the muons, A_{FB}, and the longitudinal polarization fraction of the K^{*0}, F_L. To better understand this decay, these quantities can be measured as a function of the dimuon invariant mass squared (q^2). New physics may modify any of these quantities relative to their SM values. While previous measurements by BaBar, Belle, CDF, LHCb, and CMS are consistent with the SM [1, 2, 3, 4, 5], they are still statistically limited, and more precise measurements offer the possibility to uncover physics beyond the SM. In this Proceeding, we present measurements of A_{FB}, F_L, and the differential branching fraction $d\mathcal{B}/dq^2$ from $B^0 \rightarrow K^{*0}\mu^+\mu^-$ decays, using data collected from pp collisions at the CERN LHC by the CMS experiment at a center-of-mass energy of 8 TeV. The data correspond to an integrated luminosity of 20.5 ± 0.5 fb^{-1}. All measurements are performed in q^2 bins from 1 to 19 GeV^2. The q^2 bins $8.68 < q^2 < 10.09$ GeV^2 and $12.90 < q^2 < 14.18$ GeV^2, corresponding to the $B^0 \rightarrow K^{*0}J/\psi$ and $B^0 \rightarrow K^{*0}\psi'$ decays (ψ' refers to the $\psi(2S)$), respectively, are used to validate the analysis. The former is also used to normalize the differential branching fraction.

1. CMS detector

A detailed description of the CMS detector, together with a definition of the coordinate system used and the standard kinematic variables, can be found in Ref. [7]. The main detector components used in this analysis are the silicon tracker and the muon detection systems. The silicon tracker, located in the 3.8 T field of a superconducting solenoid, consists of three pixel layers and ten strip layers (four of which have a stereo view) in the barrel region accompanied by similar endcap pixel and strip detectors on each side that extend coverage out to $|\eta| < 2.5$. For tracks with transverse momenta $1 < p_T < 10$ GeV and $|\eta| < 1.4$, the resolutions are typically 1.5% in p_T and 25–90 (45–150) μm in the transverse (longitudinal) impact parameter. Muons are measured in the range $|\eta| < 2.4$, with detection planes made using three technologies: drift tubes, cathode strip chambers, and resistive plate chambers. In addition to the tracker and muon detectors, CMS is equipped with electromagnetic and hadronic calorimeters that cover $|\eta| < 5$. Events are selected using a two-level trigger system. The first level has specialized hardware processors that use information from the calorimeters and muon systems to select the most interesting events. A high-level trigger processor farm further decreases the event rate from around 90 kHz to around 400 Hz, before data storage.

2. Reconstruction, and event selection

All events used in this analysis were recorded with the same trigger, requiring two identified muons of opposite charge to form a vertex that is displaced from the pp collision region (beamspot). The trigger required each muon to have $p_T > 3.5$ GeV, $|\eta| < 2.2$, and to pass within 2 cm of the

beam axis. The dimuon system was required to have $p_T > 6.9$ GeV, a vertex fit χ^2 probability larger than 10%, and a separation of the vertex relative to the beamspot in the transverse plane of at least 3σ. In addition, the cosine of the angle, in the transverse plane, between the dimuon momentum vector and the vector from the beamspot to the dimuon vertex was required to be greater than 0.9.

The offline reconstruction requires two muons of opposite charge and two oppositely charged hadrons. The muons are required to match those that triggered the event readout, and also to pass general muon identification requirements. These include a track matched to at least one muon segment (collection of hits in a muon chamber consistent with the passage of a charged particle), a track fit χ^2 per degree of freedom less than 1.8, hits in at least six tracker layers with at least two from the pixel detector, and a transverse (longitudinal) impact parameter with respect to the beamspot less than 3 cm (30 cm). The reconstructed dimuon system must also satisfy the same requirements that were applied in the trigger.

The hadron tracks are required to fail the muon identification criteria, have $p_T > 0.8$ GeV, and have an extrapolated distance of closest approach to the beamspot in the transverse plane greater than twice the sum in quadrature of the distance uncertainty and the beamspot transverse size. The two hadrons must have an invariant mass within 90 MeV of the accepted K^{*0} mass for either the $K^+\pi^-$ or $K^-\pi^+$ hypothesis. To remove contamination from $\phi(1020) \to K^+K^-$ decays, the invariant mass of the hadron pair must be greater than 1.035 GeV when the charged kaon mass is assigned to both hadrons.

The B^0 candidates are obtained by fitting the four charged tracks to a common vertex, and applying a vertex constraint to improve the resolution of the track parameters. The B^0 candidates must have $p_T > 8$ GeV, $|\eta| < 2.2$, vertex fit χ^2 probability larger than 10%, vertex transverse separation from the beamspot greater than 12 times the sum in quadrature of the separation uncertainty and the beamspot transverse size, and $\cos\alpha_{xy} > 0.9994$, where α_{xy} is the angle, in the transverse plane, between the B^0 momentum vector and the line-of-flight between the beamspot and the B^0 vertex. The invariant mass m of the B^0 candidate must also be within 280 MeV of the accepted B^0 mass m_{B^0} for either the $K^-\pi^+\mu^+\mu^-$ or $K^+\pi^-\mu^+\mu^-$ hypothesis. The selection criteria are optimized using simulated signal samples and background from data using sidebands of the B^0 mass. After applying the selection criteria, events in which at least one candidate is found contain on average 1.05 candidates. A single candidate is chosen from each event based on the best B^0 vertex fit χ^2.

From the selected events, the dimuon invariant mass q and its calculated uncertainty σ_q are used to distinguish the signal from the control samples. The control samples $B^0 \to K^{*0}J/\psi$ and $B^0 \to K^{*0}\psi'$ are defined by $|q - m_{J/\psi}| < 3\sigma_q$ and $|q - m_{\psi'}| < 3\sigma_q$, respectively, where $m_{J/\psi}$ and $m_{\psi'}$ are the accepted masses. The average value for σ_q is about 26 MeV. The signal sample is composed of the events that are not assigned to the J/ψ and ψ' samples. The signal sample still contains contributions from the control samples, mainly due to unreconstructed soft photons in the charmonium decay. These events will have a low q value and fall outside the selection described above. These events will also have a low m value and therefore they can be selectively removed using a combined selection on q and m. For $q < m_{J/\psi}$ ($q > m_{J/\psi}$), we require $|(m - m_{B^0}) - (q - m_{J/\psi})| > 160$ (60) MeV. For $q < m_{\psi'}$ ($q > m_{\psi'}$), we require $|(m - m_{B^0}) - (q - m_{\psi'})| > 60$ (30) MeV. The requirements are set such that less than 10% of the background events originate from the control channels.

The four-track vertex candidate is identified as a B^0 or $\overline{B^0}$ depending on whether the $K^+\pi^-$ or
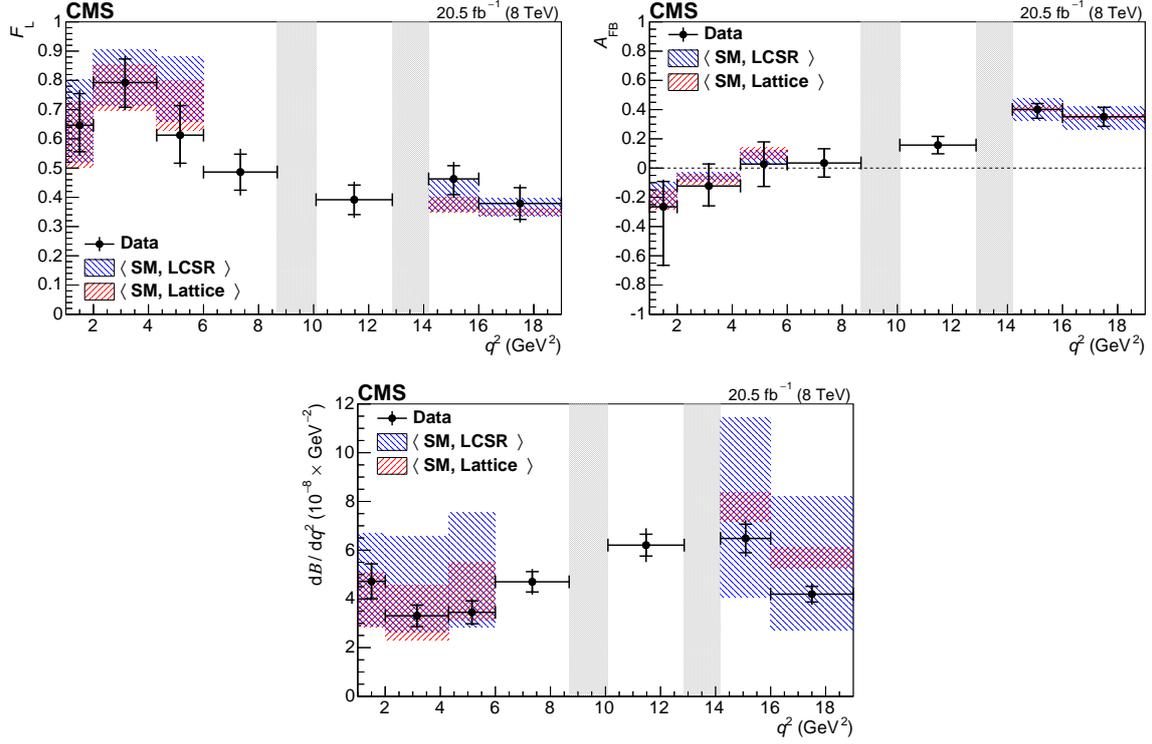
Figure 1: Measured values of F_L, A_{FB}, and $d\mathscr{B}/dq^2$ versus q^2 for $B^0 \rightarrow K^{*0}\mu^+\mu^-$. The statistical uncertainty is shown by the inner vertical bars, while the outer vertical bars give the total uncertainty. The horizontal bars show the bin widths. The vertical shaded regions correspond to the J/ψ and ψ' resonances. The other shaded regions show the two SM predictions after rate averaging across the q^2 bins to provide a direct comparison to the data. Controlled theoretical predictions are not available near the J/ψ and ψ' resonances.

$K^-\pi^+$ invariant mass is closest to the accepted K^{*0} mass. The fraction of candidates assigned to the incorrect state is estimated from simulations to be 12–14%, depending on q^2.

3. Analysis method

This analysis measures A_{FB}, F_L, and $d\mathscr{B}/dq^2$ of the decay $B^0 \rightarrow K^{*0}\mu^+\mu^-$ as a function of q^2. The angular observables needed to define the decay are: θ_K is the angle between the kaon momentum and the direction opposite to the B^0 ($\overline{B^0}$) in the K^{*0} ($\overline{K^{*0}}$) rest frame, θ_l is the angle between the positive (negative) muon momentum and the direction opposite to the B^0 ($\overline{B^0}$) in the dimuon rest frame, and ϕ is the angle between the plane containing the two muons and the plane containing the kaon and pion. As the extracted angular parameters A_{FB} and F_L do not depend on ϕ and the product of the acceptance and efficiency is nearly constant as a function of ϕ, the angle ϕ is integrated out. Although the $K^+\pi^-$ invariant mass must be consistent with that of a K^{*0}, there can be a contribution from spinless (S-wave) $K^+\pi^-$ combinations. This is parametrized with two terms: F_S, which is related to the S-wave fraction, and A_S, which is the interference amplitude

between the S-wave and P-wave decays. Including this component, the angular distribution of $B^0 \rightarrow K^{*0}\mu^+\mu^-$ can be written as:

$$\frac{1}{\Gamma}\frac{d^3\Gamma}{d\cos\theta_K d\cos\theta_l dq^2} = \frac{9}{16}\left(\frac{2}{3}\left(F_S + A_S\cos\theta_K\right)(1-\cos^2\theta_l)+ \right.$$
$$+(1-F_S)\left[2F_L\cos^2\theta_K(1-\cos^2\theta_l)+\right.$$
$$+\frac{1}{2}(1-F_L)(1-\cos^2\theta_K)(1+\cos^2\theta_l)+$$
$$\left.\left.+\frac{4}{3}A_{FB}(1-\cos^2\theta_K)\cos\theta_l\right]\right). \tag{3.1}$$

For each q^2 bin, the observables of interest are extracted from an unbinned extended maximum-likelihood fit to three variables: the $K^+\pi^-\mu^+\mu^-$ invariant mass m and the two angular variables θ_K and θ_l. For each q^2 bin, the probability density function (PDF) has the following expression:

$$\text{PDF}(m,\theta_K,\theta_l) = Y_S^C\left[S^C(m)\,S^a(\theta_K,\theta_l)\,\varepsilon^C(\theta_K,\theta_l)\right.$$
$$\left.+\frac{f^M}{1-f^M}\,S^M(m)\,S^a(-\theta_K,-\theta_l)\,\varepsilon^M(\theta_K,\theta_l)\right]$$
$$+Y_B\,B^m(m)\,B^{\theta_K}(\theta_K)\,B^{\theta_l}(\theta_l), \tag{3.2}$$

where the contributions correspond to correctly tagged signal events, mistagged signal events, and background events. The parameters Y_S^C and Y_B are the yields of correctly tagged signal events and background events, respectively, and are free parameters in the fit. The parameter f^M is the fraction of signal events that are mistagged and is determined from MC simulation. The signal mass probability functions $S^C(m)$ and $S^M(m)$ are each the sum of two Gaussian functions and describe the mass distribution for correctly tagged and mistagged signal events, respectively. In the fit, there is one free parameter for the mass value in both signal functions, while the other parameters (four Gaussian σ parameters and two fractions relating the contribution of each Gaussian) are obtained from MC simulation. The function $S^a(\theta_K,\theta_l)$ describes the signal in the two-dimensional (2D) space of the angular observables and corresponds to Eq. (3.1). The combination $B^m(m), B^{\theta_K}(\theta_K), B^{\theta_l}(\theta_l)$ is obtained from B^0 sideband data and describes the background in the space of (m,θ_K,θ_l), where the mass distribution is an exponential function and the angular distributions are polynomials ranging from second to fourth degree, depending on the q^2 bin and the angular variable. The functions $\varepsilon^C(\theta_K,\theta_l)$ and $\varepsilon^M(\theta_K,\theta_l)$ are the efficiencies, determined from MC, in the 2D space of the angular observables for correctly tagged and mistagged signal events, respectively.

4. Results

The signal data, corresponding to 1430 signal events, are fit in seven disjoint q^2 bins from 1 to 19 GeV^2. Results are also obtained for a wide, low-q^2 bin ($1 < q^2 < 6$ GeV^2), where the theoretical uncertainties are best understood. These results are shown in Fig. 1, along with two

SM predictions. The F_S fitted values are all less than 0.1%, with positive statistical uncertainties ranging from 2% to 14%. The values for A_S vary from -0.5 to $+0.3$, with statistical uncertainties of ±0.2 to ±0.3.

The SM predictions are derived from Refs. [8, 9]. The two SM predictions differ in the calculation of the form factors: the light-cone sum rules (LCSR) calculation is made at low q^2 and is extrapolated to high q^2, and the lattice gauge (Lattice) calculation of the form factors.
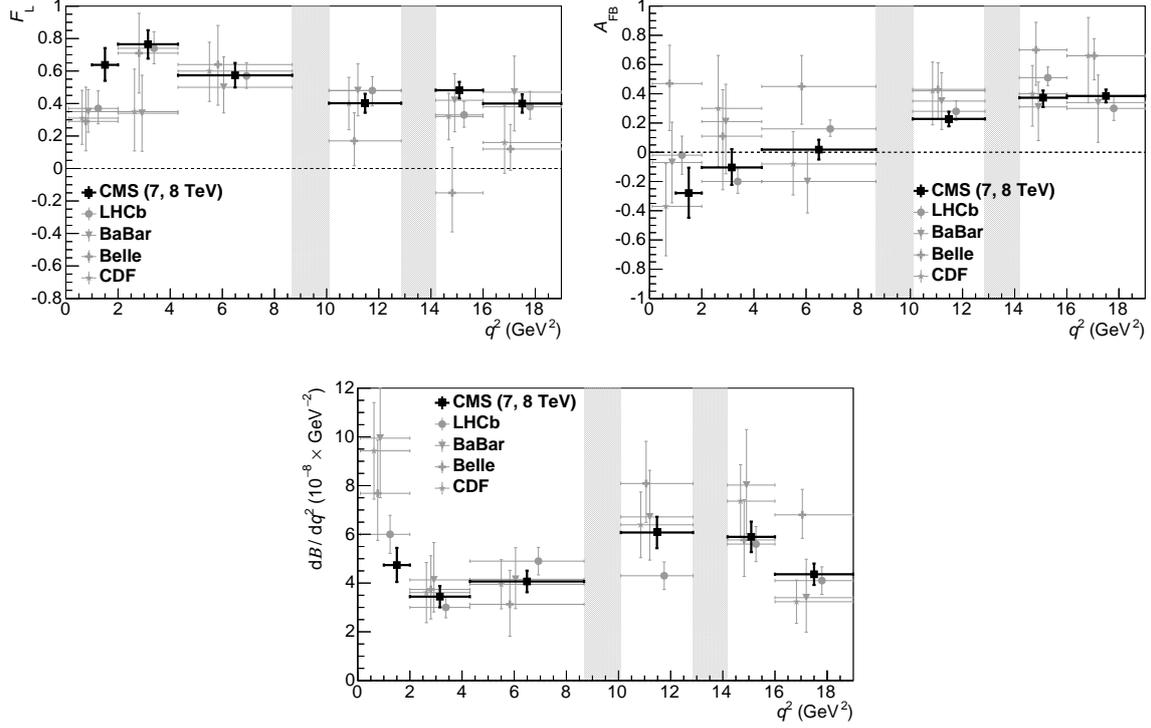
Figure 2: Measured values of F_L, A_{FB}, and $d\mathscr{B}/dq^2$ for $B^0 \to K^{*0}\mu^+\mu^-$ from CMS (combination of the 7 TeV [5] results and this analysis), BaBar [1], Belle [2], CDF [3], and LHCb [4]. The CMS and LHCb results are from $B^0 \to K^{*0}\mu^+\mu^-$ decays. The remaining experiments add the corresponding B^+ decay, and the BaBar and Belle experiments also include the dielectron mode. The vertical bars give the total uncertainty. The horizontal bars show the bin widths. The horizontal positions of the data points are staggered to improve legibility. The vertical shaded regions correspond to the J/ψ and ψ' resonances.

The results described are combined with previous CMS measurements, obtained from an independent data sample collected at $\sqrt{s} = 7$ TeV [5]. To account for the asymmetric uncertainties, the linear variance method from Ref. [10] is used. The combined CMS measurements of A_{FB}, F_L, and the differential branching fraction versus q^2 are compared to previous measurements [1, 2, 3, 4, 5] in Fig. 2. The CMS measurements are consistent with the other results, with comparable or higher precision. Table 1 provides a comparison of the measured quantities in the low dimuon invariant mass region: $1 < q^2 < 6$ GeV^2, as well as the corresponding theoretical calculations.

A more detailed description of the analysis can be found in Ref. [6].

Table 1: Measurements from CMS (the 7 TeV results [5], this work for 8 TeV, and the combination), BaBar [1], Belle [2], CDF [3], and LHCb [4] of F_L, A_{FB}, and $d\mathcal{B}/dq^2$ in the region $1 < q^2 < 6\,\mathrm{GeV^2}$ for the decay $B^0 \to K^{*0}\mu^+\mu^-$. The CMS and LHCb results are from $B^0 \to K^{*0}\mu^+\mu^-$ decays. The remaining experiments add the corresponding B^+ decay, and the BaBar and Belle experiments also include the dielectron mode. The first uncertainty is statistical and the second is systematic. For the combined CMS results, only the total uncertainty is reported. The two SM predictions are also given.

Sw

Experiment	F_L	A_{FB}	$d\mathcal{B}/dq^2$ ($10^{-8}\,\mathrm{GeV^{-2}}$)
CMS (7 TeV)	$0.68 \pm 0.10 \pm 0.02$	$-0.07 \pm 0.12 \pm 0.01$	$4.4 \pm 0.6 \pm 0.4$
CMS (8 TeV, this analysis)	$0.72 \pm 0.05 \pm 0.04$	$-0.15^{+0.10}_{-0.08} \pm 0.03$	$3.6 \pm 0.3 \pm 0.3$
CMS (7 TeV + 8 TeV)	0.71 ± 0.06	$-0.12^{+0.07}_{-0.08}$	3.8 ± 0.4
LHCb	$0.65^{+0.08}_{-0.07} \pm 0.03$	$-0.17 \pm 0.06 \pm 0.01$	$3.4 \pm 0.3^{+0.4}_{-0.5}$
BaBar	—	—	$4.1^{+1.1}_{-1.0} \pm 0.1$
CDF	$0.69^{+0.19}_{-0.21} \pm 0.08$	$0.29^{+0.20}_{-0.23} \pm 0.07$	$3.2 \pm 1.1 \pm 0.3$
Belle	$0.67 \pm 0.23 \pm 0.05$	$0.26^{+0.27}_{-0.32} \pm 0.07$	$3.0^{+0.9}_{-0.8} \pm 0.2$
SM (LCSR)	$0.79^{+0.09}_{-0.12}$	$-0.02^{+0.03}_{-0.02}$	$4.6^{+2.3}_{-1.7}$
SM (Lattice)	$0.73^{+0.08}_{-0.10}$	$-0.03^{+0.04}_{-0.03}$	$3.8^{+1.2}_{-1.0}$

5. Conclusions

Using pp collision data recorded at $\sqrt{s} = 8$ TeV with the CMS detector at the LHC, corresponding to an integrated luminosity of 20.5 fb^{-1}, an angular analysis has been carried out on the decay $B^0 \to K^{*0}\mu^+\mu^-$. The data used for this analysis include 1430 signal decays. For each bin of the dimuon invariant mass squared (q^2), unbinned maximum-likelihood fits were performed to the distributions of the $K^+\pi^-\mu^+\mu^-$ invariant mass and two decay angles, to obtain values of the forward-backward asymmetry of the muons, A_{FB}, the fraction of longitudinal polarization of the K^{*0}, F_L, and the differential branching fraction, $d\mathcal{B}/dq^2$. The results are among the most precise to date and are consistent with standard model predictions and previous measurements.

References

[1] BaBar collaboration, *Angular distributions in the decay $B \to K^*\ell^+\ell^-$*, Phys. Rev. D **79**, 031102 (2009)

[2] Belle collaboration, *Measurement of the differential branching fraction and forward-backward asymmetry for $B \to K^{(*)}\ell^+\ell^-$*, Phys. Rev. Lett. **103**, 171801 (2009)

[3] CDF collaboration, *Differential branching fraction and angular analysis of the decay $B^0 \to K^{*0}\mu^+\mu^-$*, Phys. Rev. D **108**, 181806 (2009)

[4] LHCb collaboration, *Differential branching fraction and angular analysis of the decay $B^0 \to K^{*0}\mu^+\mu^-$*, JHEP **08**, 131 (2013)

[5] CMS collaboration, *Angular analysis and branching fraction measurement of the decay $B^0 \to K^{*0}\mu^+\mu^-$*, Phys. Lett. B **727**, 77 (2013)

[6] CMS collaboration, *Angular analysis of the decay $B^0 \to K^{*0}\mu^+\mu^-$ from pp collisions at $\sqrt{s} = 8$ TeV*, arXiv **1507.08126** (2015)

[7] CMS collaboration, *The CMS experiment at the CERN LHC*, *JINST* **3**, S08004 (2008)

[8] Bobeth, C. and Hiller, G. and van Dyk, D., *The benefits of $\overline{B} \to \overline{K}^* \ell^+ \ell^-$ decays at low recoil*, *JHEP* **07**, 098 (2010)

[9] Bobeth, C. and Hiller, G. and van Dyk, D., *General analysis of $\overline{B} \to \overline{K}^{(*)} \ell^+ \ell^-$ decays at low recoil*, *Phys. Rev. D* **87**, 034016 (2012)

[10] Barlow, R., *Asymmetric statistical errors*, *arXiv* **physics/0406120** (2006)